BJP British Journal of Pharmacology

DOI:10.1111/j.1476-5381.2011.01206.x
www.brjpharmacol.org

RESEARCH PAPER

Astragaloside IV synergizes with ferulic acid to inhibit renal tubulointerstitial fibrosis in rats with obstructive nephropathy

LQ Meng[1], JW Tang[1], Y Wang[1], JR Zhao[1], MY Shang[2], M Zhang[1], SY Liu[1], L Qu[1], SQ Cai[2] and XM Li[1]*

[1]*Renal Division, Department of Medicine, Peking University First Hospital; Peking University Institute of Nephrology; Key Laboratory of Renal Disease, Ministry of Health of China, Beijing, China, and* [2]*State Key Laboratory of Natural and Biomimetic Drugs, Peking University School of Pharmaceutical Sciences, Beijing, China*

Correspondence
Professor Xiaomei Li, Renal Division, Department of Medicine, Peking University First Hospital, No. 8 Xishiku Street Xicheng District, Beijng China.
E-mail: xiaomei0708@gmail.com

Keywords
astragaloside IV; ferulic acid; renal tubulointerstitial fibrosis; mitogen-activated protein kinase; unilateral ureteral obstruction; rat; Astragali Radix; Angelicae Sinensis Radix

Received
27 June 2010
Revised
28 November 2010
Accepted
1 December 2010

BACKGROUND AND PURPOSE
The combination of Chinese herbs, Astragali Radix and Angelicae Sinensis Radix, could alleviate renal interstitial fibrosis. Astragaloside IV (AS-IV) and ferulic acid (FA) are the two major active constituents in this combination. In this study, we employed rats with unilateral ureteral obstruction to determine whether AS-IV and FA have the same renoprotective effects and investigated the mechanisms of this action.

EXPERIMENTAL APPROACH
Renal pathological changes were evaluated after treatment with AS-IV, FA or AS-IV + FA (*AF*) for 10 days. Meanwhile, the expression of transforming growth factor β_1 (TGF-β_1), fibronectin, α-smooth muscle actin (α-SMA), phosphorylation of c-Jun NH_2-terminal kinase (p-JNK) and nitric oxide (NO) production in kidney were determined. The expressions of fibronectin, α-SMA, mitogen-activated protein kinases [JNK, extracellular signal-regulated kinases (ERK), P38] in TGF-β_1-treated NRK-49F cells or interleukin-1-treated HK-2 cells after AS-IV, FA or *AF* were assessed.

KEY RESULTS
AF alleviated the infiltration of mononuclear cells, tubular atrophy and interstitial fibrosis; reduced the expression of fibronectin, α-SMA, TGF-β_1 and p-JNK; and dramatically increased the production of NO in obstructed kidneys. Neither AS-IV nor FA alone improved renal damage, but both increased NO production. *AF* inhibited α-SMA and fibronectin expression in NRK-49F or HK-2 cells. Furthermore, *AF* significantly inhibited IL-1β-induced JNK phosphorylation, without affecting ERK or P38 phosphorylation. Neither AS-IV nor FA alone had any effect on the cells.

CONCLUSIONS AND IMPLICATIONS
AS-IV synergizes with FA to alleviate renal tubulointerstitial fibrosis; this was associated with inhibition of tubular epithelial–mesenchymal transdifferentiation (EMT) and fibroblast activation, as well as an increase in NO production in the kidney.

Abbreviations
A&A, the mixture of Astragali Radix and Angelicae Sinensis Radix; *AF*, the combination of astragaloside IV and ferulic acid; AS-IV, astragaloside IV; CKD, chronic kidney disease; ECM, extracellular matrix; FA, ferulic acid; IL-1, interleukin-1; MAPK, mitogen-activated protein kinase; TGF-β_1, transforming growth factor-β_1; UUO, unilateral ureteral obstruction; α-SMA, α-smooth muscle actin

Introduction

Chronic kidney disease (CKD) is widely recognized as a major public health problem that progressively develops to end-stage renal disease (ESRD) irrespective of the underlying cause. The persistent kidney injury induces renal inflammation, the overexpression of profibrotic factors and myofibroblast proliferation, followed by an exaggerated accumulation of extracellular matrix (ECM) components, destruction of the renal vasculature and ultimately renal fibrosis (Hewitson, 2009). Although the systematic approach used to treat this condition includes intensive reduction of blood pressure and dietary restriction, this is not effective enough to completely halt the progression of CKD (Ripley, 2009).

It is well accepted that tubulointerstitial fibrosis is a better indicator of the deterioration of renal function than glomerulosclerosis in renal diseases (Bohle *et al.*, 1987). Inhibition of tubulointerstitial fibrosis has the potential to protect the kidney from the deleterious effects of CKD. In the progression of CKD, the activated interstitial fibroblast or myofibroblast is central to the development of tubulointerstitial fibrosis (Strutz and Zeisberg, 2006). A number of pro-inflammatory, profibrotic cytokines, such as transforming growth factor-β_1 (TGF-β_1) (Schnaper *et al.*, 2009), interleukin-1 (Fan *et al.*, 2001; Vesey *et al.*, 2002) and connective tissue growth factor (Chen *et al.*, 2009), as well as angiotensin II (Gaedeke *et al.*, 2002) are released from the kidney in pathological conditions. These factors converge and establish a fibrogenic context that drives the resident cells, including fibroblasts (Qi *et al.*, 2006), pericytes (Lin *et al.*, 2008), tubular cells (Kalluri and Neilson, 2003) and endothelial cells (Zeisberg *et al.*, 2008), to transform into myofibroblasts. The number of myofibroblasts is closely associated with the extent of tubulointerstitial fibrosis (Qi *et al.*, 2006). Therefore, to intervene in the transition of these cellular phenotypes is pivotal in inhibiting tubulointerstitial fibrosis.

In China, many Chinese herbal medicines have been reported to slow down the progression of CKD (Li and Wang, 2005; Peng *et al.*, 2005; Wojcikowski *et al.*, 2006), including Astragali Radix [the root of *Astragalus membranaceus* (Fisch.) Bge. var. *mongholicus* (Bge.) Hsiao] and Angelicae Sinensis Radix [the root of *Angelia sinensis* (Oliv.) Diels]. The combination of Astragali Radix and Angelicae Sinensis Radix was demonstrated to possess a renoprotective effect in animal models of CKD (Li *et al.*, 1998; Wang *et al.*, 2004; Zhang *et al.*, 2006a; Meng *et al.*, 2007; Song *et al.*, 2009), and this was associated with a down-regulation of the expression of TGF-β_1, inhibition of the epithelial–mesenchymal transdifferentiation (EMT), reduction of macrophage infiltration and myofibroblast proliferation, as well as an improvement in endothelial dysfunction.

There are about 150 components in the decoction of Astragali Radix and Angelicae Sinensis Radix (Xiao *et al.*, 1999). To identify the chemicals responsible for its renoprotective effects, we gradually refined the mixture of the two herbs according to its ability to improve the renal pathological damage (Zhao *et al.*, 2010). Using mass spectrometry analysis, we identified two major constituents, astragaloside IV (AS-IV) and ferulic acid (FA), from an extract of Astragali Radix and Angelicae Sinensis Radix, which preserve the antifibrotic effects in rats with unilateral ureteral obstruction (UUO). AS-IV was reported to inhibit the adhesion of glomerular podocyte dysfunction (Chen *et al.*, 2008), alleviate tumor necrosis factor α (TNF-α)-induced endothelial cell apoptosis (Xu *et al.*, 2006) and improve the barrier function of the endothelial cell (Qu *et al.*, 2009). FA alleviates renal injury by decreasing urinary protein excretion and inhibiting the overexpression of TGF-β_1 (Fujita *et al.*, 2008). Thus, AS-IV and FA may be the important active constituents for inhibiting tubulointerstitial fibrosis. In this study, we sought to identify the renal protective efficacy of AS-IV and FA in obstructive nephropathy and to assess the potential mechanisms of its renoprotective effects.

Methods

Drug preparation

AS-IV (Lot No. 110781-200512) and FA (Lot No. 0773-9910) used in this study were of high purity (99%) as determined by high performance liquid chromatography (HPLC) analysis and were purchased from the National Institute for the Control of Pharmaceutical and Biological Products (Beijing, China). The compounds used in the cellular experiments were dissolved in 1% DMSO (Sigma-Aldrich, St. Louis, MO, USA) in a concentration of 2 mg·mL^{-1} as a stock solution. The stock solution was diluted with incubation medium when used. The compounds were prepared as a suspension in the medium before administration to the animals. We have abbreviated the combination of AS-IV and FA to *AF* throughout the manuscript. The mixture of Astragali Radix and Angelicae Sinensis Radix (A&A) was prepared according to the protocol in our earlier study (Meng *et al.*, 2007). The quality of A&A was controlled by HPLC-electrospray ionization and mass spectrometry (Meng *et al.*, 2010).

Animal and experimental protocol

All experiments were performed with approval from the Animal Experimentation Ethics Committee of Peking University First Hospital. Male SPF Wistar rats (192 ± 8 g) were obtained from the Institute of Laboratory Animal Science, Chinese Academy of Medical Sciences (Beijng). Animals were allowed free access to water and standard rat chow. Animals were housed at 25°C with 40% humidity with a 12/12 h light/dark cycle. Animals were randomly divided into eight groups as shown in Table 1. For the UUO groups, rats were anaesthetized with sodium pentobarbital (40 mg·kg^{-1}, i.p.), then the left ureter was exposed using a mid-abdominal incision and ligated with 3-0 silk suture. In sham-operated rats, the ureter was mobilized but not ligated. The test compounds were administered to the rats by gavage on the day of the operation. Because 0.45–0.85 mg AS-IV and 0.2–0.5 mg FA were determined·per gram dried weight of A&A, the low dose and high dose of AS-IV and FA used in this study are equivalent to the minimum and maximum contents determined in A&A.

Rats from each group were killed on day 10 after surgery. Serum was obtained from the abdominal aorta blood after centrifugation to detect serum creatinine and urea using a Beckman Coulter LX20 Automated Analyzer (Beckman Coulter Inc, Brea, CA, USA). The left kidneys were decapsulated, washed with ice-cold normal saline, then rapidly dissected. Coronal sections of 2–3 mm thick through the

Table 1
The groups of rats and their administrations in animal experiments

Group	Abbreviation	Administration
Sham-operated	Sham	Deionized water 3 mL·d^{-1}
Unilateral ureteral obstruction	UUO	Deionized water 3 mL·d^{-1}
UUO + enalapril treatment	Enalapril	Enalapril: 4 mg·kg^{-1}·d^{-1}
UUO + A&A treatment	A&A	A&A: 12 g·kg^{-1}·d^{-1}
UUO + low-dose (AS-IV + FA) treatment	*AF*-L	AS-IV: 10.8 mg·kg^{-1}·d^{-1} + FA 4.8 mg·kg^{-1}·d^{-1}
UUO + high-dose (AS-IV + FA) treatment	*AF*-H	AS-IV: 20.4 mg·kg^{-1}·d^{-1} + FA 12 mg·kg^{-1}·d^{-1}
UUO + AS-IV treatment	AS-IV	AS-IV: 10.8 mg·kg^{-1}·d^{-1}
UUO + FA treatment	FA	FA: 4.8 mg·kg^{-1}·d^{-1}

mid-portion of kidney were embedded in paraffin after being fixed in 10% neutral buffered formalin; the rest was snap froze in liquid nitrogen for further study.

Cell culture

Rat renal fibroblasts (NRK-49F) were obtained from ATCC (Manassas, VA). Cells were used between passages 3 and 15. The cells were grown in culture dishes and maintained in Dulbecco's modified Eagle's medium (DMEM) supplemented with 10% fetal bovine serum (FBS) (Hyclone, Logan, UT) and 100 U·mL^{-1} penicillin and 100 mg·mL^{-1} streptomycin. Equal numbers of NRK-49F cells (2×10^5) were cultured on 35 mm dishes until 70–80% confluence in 10% FBS-containing medium and then changed to serum-free medium for 24 h. Cells were pretreated with 0.1% DMSO, AS-IV (24 μmol·L^{-1}), FA (43 μmol·L^{-1}) and *AF* (AS-IV 24 μmol·L^{-1} + FA 43 μmol·L^{-1}), respectively, for 30 min and then stimulated with TGF-β_1 (1 ng·mL^{-1}) or incubation medium for 24 h. Human proximal tubular epithelial cells (HK-2) were obtained from ATCC. The cells were maintained in DMEM supplemented with 10% FBS. Equal numbers of HK-2 cells (2×10^5) were cultured on 35 mm dishes until 95% confluence in 10% FBS-containing medium and then changed to 0.2% fetal calf serum–containing medium for 24 h. Cells were pretreated with 0.1% DMSO, AS-IV (24 μmol·L^{-1}), FA (43 μmol·L^{-1}) and *AF* (AS-IV 24 μmol·L^{-1} + FA 43 μmol·L^{-1}), respectively, for 30 min and then stimulated with IL-1β (10 ng·mL^{-1}) or incubation medium for 24 h.

Morphological and quantitative image analysis

Sections were stained with haematoxylin and eosin (HE) and Masson trichrome for morphological studies. Ten randomly selected separate non-overlapping microscopic fields of each kidney section were examined under the light microscope at a magnification (×200) and averaged to yield the score of each kidney. Morphometric evaluation of the tubulointerstitial area was performed by two authors under the direction of an expert in experimental renal pathology. The renal pathology of animals was assessed using a severity index (Radford *et al.*, 1997) that assigns points (0 to 3) for interstitial features of kidney. The extents of interstitial fibrosis, tubular atrophy (defined as luminal dilation and flattened tubular epithelial cells) and interstitial cell infiltration were semiquantitatively scored as absent (0), involving less than 25% of the field (1), involving 26% to 50% of the field (2) and involving greater than 50% of the field (3).

Immunohistochemistry

After formalin fixation and paraffin embedding, 4 μm sections were deparaffinized in xylene and rehydrated through graded ethanols. The endogenous peroxidase activity was suppressed by exposing slide-mounted tissue to 0.3% H_2O_2 after antigen retrieval with pepsin or boiling. Sections were then incubated with the following polyclonal antibodies overnight at 4°C in phosphate-buffered saline: TGF-β_1 (Santa Cruz Biotechnology, Santa Cruz, CA, USA), fibronectin (Santa Cruz Biotechnology), α-SMA (Zymed Laboratories, San Francisco, CA, USA). After being washed, slides were incubated with biotinylated goat anti-rabbit IgG antibody and then peroxidase conjugated streptavidin. Sections were visualized with diaminobenzidine tetrahydrochloride (DAB) substrate and counterstained with haematoxylin.

The expression of TGF-β_1, fibronectin or α-SMA in cortical interstitium was assessed by spectrophotometry. The stained sections were visualized on a computer display with an Olympus DP50 camera connected to a light Olympus BX51 microscope (Olympus Optical Co., Tokyo, Japan) at an original magnification of ×200. The morphometric evaluation consisted of quantitative analyses of TGF-β_1, fibronectin or α-SMA by using specific software (Image-Pro Plus 6.0, Media Cybernetics Inc. Bethesda, MD, USA). At least ten non-overlapping fields at a magnification of ×200 per section were analysed for each animal. The expression of TGF-β_1, fibronectin or α-SMA was assessed by the ratio of the mean positively stained area to the mean whole area of the section.

Immunofluorescence

After formalin fixation and paraffin embedding, 4 μm sections were deparaffinized in xylene and rehydrated through graded ethanols. Sections were then incubated with a mouse monoclonal antibody of phosphorylation of c-Jun NH_2-terminal kinase (p-JNK, Santa Cruz Biotechnology) overnight at 4°C in PBS. After being washed, slides were incubated with

tetraethyl rhodamine isothiocyanate-labelled goat anti-mouse IgG antibody. All sections were counterstained with 4′,6-diamidino-2-phenylindole.

Determination of renal tissue nitric oxide (NO)

Kidney tissue (~100 mg) was pulverized using a chilled mortar and pestle and then resuspended in 3 mL modified radioimmunoprecipitation assay buffer containing 50 mM Tris–HCl (pH 7.4), 1% NP-40, 0.25% Na deoxycholate, 150 mM NaCl, 1 mM EDTA, 1 mM phenylmethanesulphonyl fluoride, 1 μg·mL^{-1} aprotinin, 1 μg·mL^{-1} leupeptin, 1 μg·mL^{-1} pepstatin, 1 mM Na_3VO_4, and 1 mM NaF. After being incubated at 4°C for 1 h, the suspension was centrifuged (22 000× *g*, 4°C, 30 min), and the supernatant was aliquoted, frozen in liquid nitrogen and stored at –80°C until use. The measurement of NO in kidney homogenates was performed according to a method described previously (Meng *et al.*, 2007). Briefly, 100 μL of the supernatant of kidney homogenates was incubated with nitrate reductase, which converted nitrate to nitrite, for 1 h at 37°C. Then, the samples were incubated for 10 min at room temperature after the addition of the Griess reagent. The optical density values of the samples were measured at 530 nm on a spectrophotometer (Beckman DU530, Beckman Coulter Inc, Brea, CA, USA). The concentration of total nitrite, expressed as μmol·mg^{-1} protein, represented NO production in the homogenates.

Western blot analysis

Proteins in cell lysates were analysed by sodium dodecyl sulphate–polyacrylamide gel electrophoresis (SDS–PAGE) and then electrophoretically transferred to nitrocellulose membrane. The nitrocellulose membrane was blocked with 5% skimmed milk in Tris-buffered saline–Tween-20 (TBS-T) for 1 h. The membrane was incubated with antibodies for α-SMA, fibronectin and mitogen-activated protein kinases (MAPKs) diluted in 2% (w/v) BSA dissolved in TBS-T at 4°C overnight. Blots were washed for 45 min in TBS-T before incubation with a horseradish peroxidase (HRP)–conjugated anti-rabbit or anti-mouse IgG for 2 h at room temperature with rotation. Proteins were detected on X-ray film using chemiluminescence reagent plus (Perkin-Elmer Life Sciences, Waltham, MA, USA).

RNA extraction and quantitative reverse transcription–PCR analysis

Total RNA was isolated from the cultured cells by a simple Total RNA Kit (Tinagen, Beijing, China) according to the manufacturer's instructions. Template cDNA was prepared using a Reverse Transcription System A3500 (Promega, Madison, WI) and quantified by real-time PCR using the FastStart Universal SYBR Green Master (ROX) (Roche, Indianapolis, IN), with glyceraldehyde-3-phosphate dehydrogenase (GAPDH) as an endogenous control for normalization. Quantitative real-time PCR was performed using an ABI Prism 7500 Sequence Detection System (Applied Biosystems, Life Technologies, Carlsbad, CA, USA). Briefly, 1 μg of total RNA was reverse-transcribed and subjected to PCR as follows: 95°C for 10 min followed by 40 cycles at 95°C for 15 s, 60°C for 1 min. The primers used in this study were shown in Table 2.

Table 2

The primers of α-SMA, fibronectin and GAPDH

Genes	Primers
α-SMA	
Sense	5′-CTTCCAGCCATCTTTCATTGG-3′
Antisense	5′-ATATCACACTTCATGATGCTGTTATAGGT-3′
Fibronectin	
Sense	5′-TTATGACGACGGGAAGACCT-3′
Antisense	5′-GCTGGATGGAAAGATTACTC-3′
GAPDH	
Sense	5′-TGCACCACCAACTGCTTAGC-3′
Antisense	5′-GGCATGGACTGTGGTCATGAG-3′

Reaction specificity was confirmed by melting curve analysis. Gene expression profiles were normalized to GAPDH and calculated using the ΔΔCt ($2^{-\Delta\Delta Ct}$) method for each sample.

Statistical analysis

Results are expressed as mean ± SD. The results were assessed by one-way analysis of variance (ANOVA) for comparisons among groups. Differences between groups were determined by Tukey's multiple comparisons tests. Results were considered significant when $P < 0.05$. All analyses were performed with the SPSS14.0 statistical software package (SPSS Inc., Chicago, IL, USA).

Results

AF improved renal function and renal interstitial injury

The serum creatinine and urea levels were higher in the UUO group than that in the sham control group ($P < 0.05$) and were all decreased after treatment with Enalapril, A&A, *AF*-H or *AF*-L ($P < 0.05$). There was no difference between the AS-IV or FA alone treated group and the UUO group. As shown in Figure 1 and Table 3, the semiquantitative histomorphometry analysis on HE- and Masson-stained sections revealed significant infiltration of mononuclear cells, damaged tubules and interstitial fibrosis in the obstructed kidneys, compared with that in sham controls ($P < 0.05$). The pathological changes were significantly alleviated by *AF* (high or low dose), with similar effects obtained with Enalapril or A&A ($P < 0.05$), but there was no significant change after treatment with either AS-IV or FA alone.

AF alleviated the expression of fibronectin, α-SMA, TGF-β_1 in obstructed kidneys

We examined the interstitial fibronectin accumulation in fibrotic kidney after AS-IV and FA treatment. As a major component of the ECM in the fibrotic kidney, fibronectin was prominently stained in the tubulointerstitium of obstructed kidneys compared with the sham-operated kidneys. The

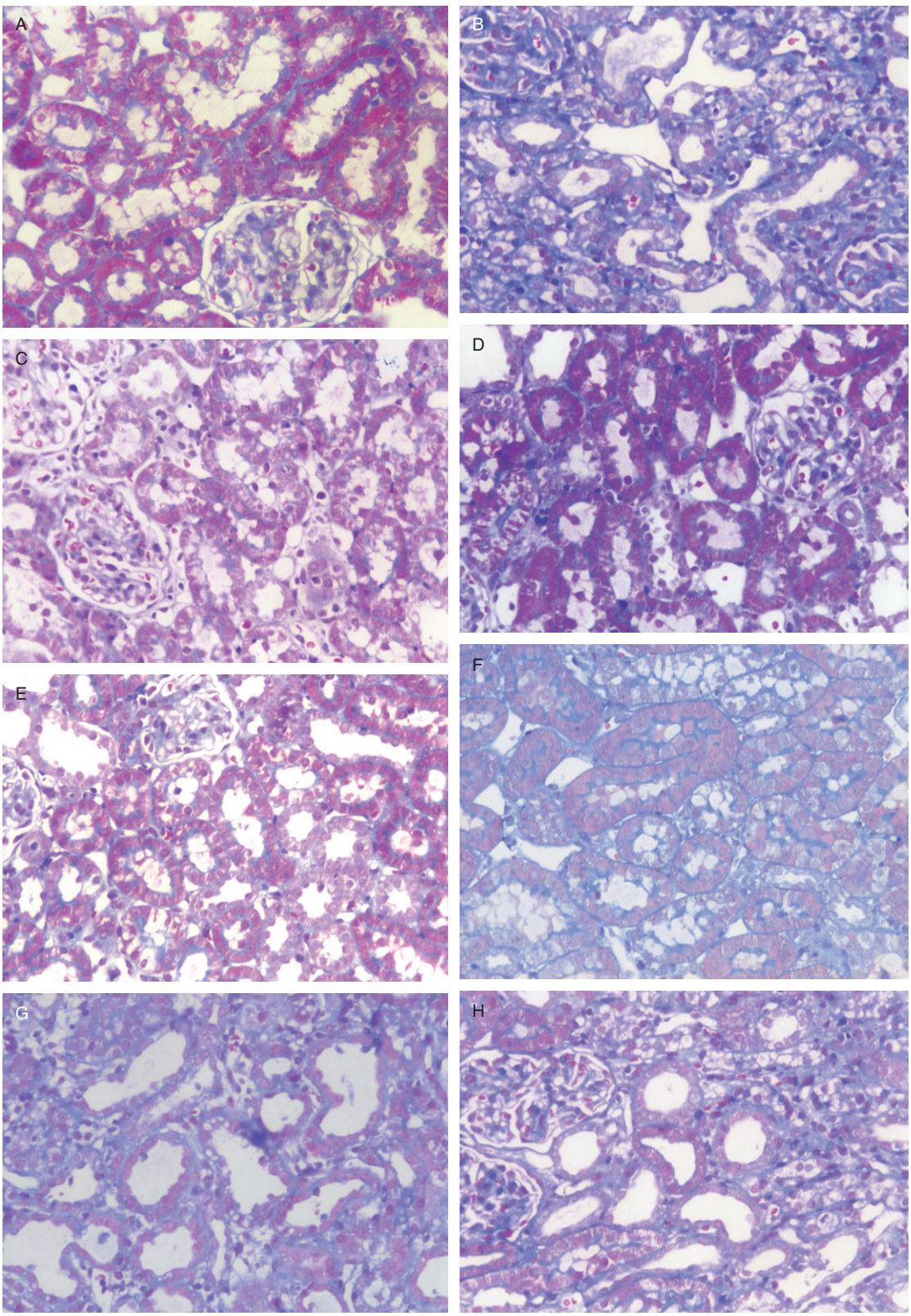

Figure 1

Renal tubulointerstitial damage in obstructed kidneys. (A) Sham group. (B) UUO group. (C) UUO + Enarapril treatment. (D) UUO + A&A treatment. (E) UUO + AF-L treatment. (F) UUO + AF-H treatment. (G) UUO + AS-IV treatment. (H) UUO + FA treatment. UUO: unilateral ureteral obstruction, A&A: a decoction of Astragali Radix and Angelicae Sinensis Radix, AS-IV: astragaloside IV, FA: ferulic acid, AF-L: AS-IV & FA (low dose), AF-H: AS-IV & FA (high dose).

Table 3

Renal function and tubulointerstitial injury of obstructed kidney in rats

Group	*n*	Creatinine (μmol·L^{-1})	Urea (mmol·L^{-1})	Tubulointerstitial injury index
Sham + vehicle	3	35.67 ± 1.53	4.70 ± 0.26	0.86 ± 0.17
UUO + vehicle	3	72.33 ± 4.50*	8.64 ± 1.47*	9.70 ± 0.95*
UUO + Enalapril	8	59.63 ± 7.37*#	7.81 ± 1.39*#	4.98 ± 0.88*#
UUO + A&A	8	51.36 ± 2.97*#	6.92 ± 1.95*#	6.95 ± 0.95*#
UUO + *AF*-L	8	48.50 ± 3.42*#	6.70 ± 0.56*#	5.97 ± 1.07*#
UUO + *AF*-H	8	49.00 ± 6.87*#	6.30 ± 0.80*#	5.62 ± 1.23*#
UUO + AS-IV	8	63.87 ± 10.45*	8.67 ± 1.32*	7.95 ± 1.61*
UUO + FA	8	62.25 ± 5.87*	7.51 ± 0.42*	8.08 ± 1.45*

AF reduces renal tubulointerstitial injury after UUO. Cellular infiltration, tubular atrophy and interstitial fibrosis were observed 10 days after UUO. Semiquantitative scoring of tubulointerstitial injury revealed more damage in UUO than in sham–treated kidneys and was improved after treatment of enalapril, A&A or *AF*. Data are expressed as means ± SD.
*$P < 0.05$ versus sham-operated rats; #$P < 0.05$ versus UUO kidneys treated with vehicle.
UUO, unilateral ureteral obstruction; A&A, a decoction of Astragali Radix and Angelicae Sinensis Radix; AS-IV, astragaloside IV; FA, ferulic acid; *AF*-L, AS-IV & FA (low dosage); *AF*-H, AS-IV & FA (high dosage).

semiquantitative histomorphometric analysis showed that obstructive injury provoked a 7.5-fold induction of fibronectin ($P < 0.05$). Monotherapy with AS-IV or FA alone did not attenuate the accumulation of fibronectin, but *AF* treatment resulted in a significant reduction of fibronectin ($P < 0.05$, Figure 2).

The expression of α-SMA is the molecular hallmark of myofibroblasts. As shown in Figure 2, α-SMA was expressed in the smooth muscle cells of renal arterioles but was rarely evident in the tubulointerstitium of sham-operated kidneys. Quantification of immunostaining in renal tissue indicated a striking increase in the α-SMA-positive area in the obstructed kidneys compared with that in the sham control ($P < 0.05$), and treatment with *AF* significantly reduced interstitial expression of α-SMA ($P < 0.05$).

TGF-β_1 is an important pro-fibrotic growth factor in the progression of interstitial fibrosis. As shown in Figure 2, there was only occasional immunostaining of TGF-β_1 in the tubular cells of the sham-operated kidneys but diffuse staining in the obstructive kidneys, especially the proximal tubular cells and infiltrating monocyte/macrophage. The expression of TGF-β_1 in the *AF* group was low in the epithelial cells of the dilated tubuli. Semiquantitative analysis revealed that the expression of TGF-β_1 was significantly increased in the UUO group compared with the sham group ($P < 0.05$) and was decreased after *AF* therapy compared with the UUO group ($P < 0.05$). Similar to fibronectin, AS-IV or FA treatment alone has no impact on the expression of α-SMA and TGF-β_1.

AF increased renal tissue NO production

Astragali Radix and Angelicae Sinensis Radix increased the production of NO in obstructive kidneys via enhancement of endothelial NOS activity (Meng *et al.*, 2007). In this study, we also evaluated the effect of *AF* on NO production. Figure 3 shows that the production of NO in obstructed kidney was slightly increased compared with the sham controls, but this was not statistically significant. Monotherapy with AS-IV or FA and the combination of the two constituents (*AF*) all markedly increased the production of NO in obstructed kidneys ($P < 0.05$).

AF inhibited TGF-β_1-induced α-SMA and fibronectin expression in NRK-49F cells

During ureteral obstruction, interstitial fibroblasts are activated resulting in massive proliferation and excessive ECM accumulation. In this study, the expression of α-SMA and fibronectin protein in NRK-49F cells after stimulation with TGF-β_1 was significantly higher than that in the cells treated with DMSO ($P < 0.05$). *AF* dramatically inhibited α-SMA and fibronectin overexpression compared with TGF-β_1-treated cells ($P < 0.05$; Figures 4 and 5), but AS-IV or FA did not affect the expression of α-SMA and fibronectin after stimulation with TGF-β_1. Furthermore, it was shown that *AF* inhibited the expression of α-SMA and fibronectin mRNA in NRK-49 cells treated with TGF-β_1 ($P < 0.05$; Figures 6 and 7).

AF inhibited IL-1β-induced α-SMA and fibronectin expression and JNK phosphorylation in HK-2 cells

IL-1β stimulates the transition of renal tubular epithelial cells to myofibroblasts via a TGF-β_1-dependent pathway (Fan *et al.*, 2001). Our previous study showed that IL-1β induced HK-2 cells to express the myocyte biomarker α-SMA through the activation of JNK and P38 signalling pathways (Zhang *et al.*, 2005). In this study, we evaluated the effects of *AF* on IL-1β-stimulated HK-2 cells. The renal tubular epithelial cells displayed typical cobblestone morphology, but IL-1β induced profound morphological changes, characterized by shape elongation, dissociation from neighbouring cells and loss of their cobblestone monolayer pattern. Simultaneous incubation of *AF* with IL-1β significantly restored the morphology

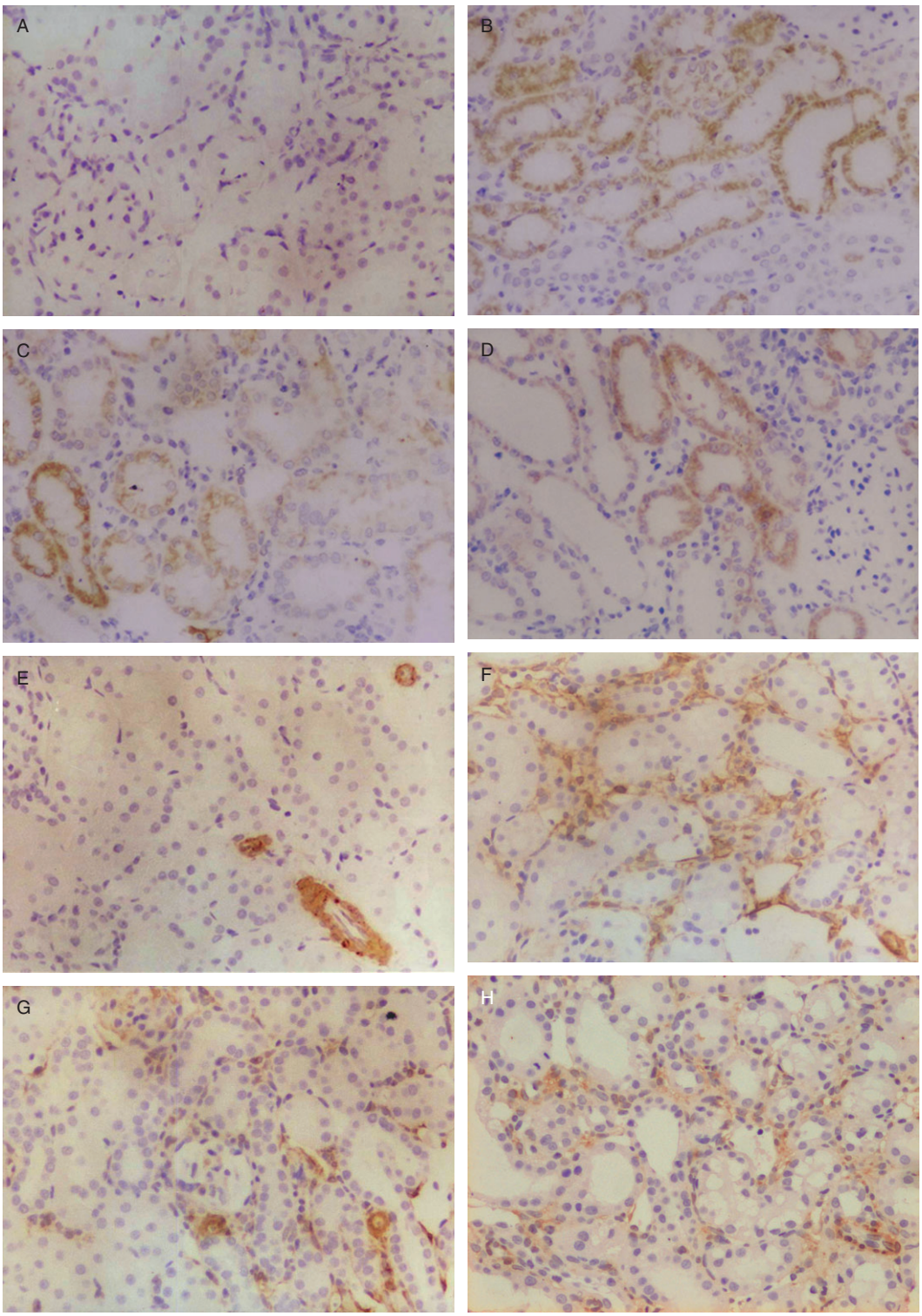

Figure 2

The expression of TGF-β1, α-SMA, fibronectin in obstructed kidneys (immunohistochemistry, 200×). (A) TGF-β1 in sham group. (B) TGF-β1 in UUO group. (C) TGF-β1 in A&A treatment group. (D) TGF-β1 in AF-L treatment group. (E) α-SMA in sham group. (F) α-SMA in UUO group. (G) α-SMA in A&A treatment group. (H) α-SMA in AF-L treatment group. (I) fibronectin in sham group. (J) fibronectin in UUO group. (K) Fibronectin in A&A treatment group. (L) Fibronectin in AF-L treatment group. (M) Semiquantitative analysis of TGF-β1, α-SMA, fibronectin expression in groups. UUO: unilateral ureteral obstruction, A&A: a decoction of Astragali Radix and Angelicae Sinensis Radix, AF-L: astragaloside IV & ferulic acid (low dose). Semiquantitative scoring of the expression of TGF-β1, α-SMA, fibronectin revealed more damage in UUO than in sham–treated kidneys, which was improved after treatment of A&A, or AF. Data are expressed as means ± SD. *$P < 0.05$ versus sham-operated rats; #$P < 0.05$ versus UUO kidneys.

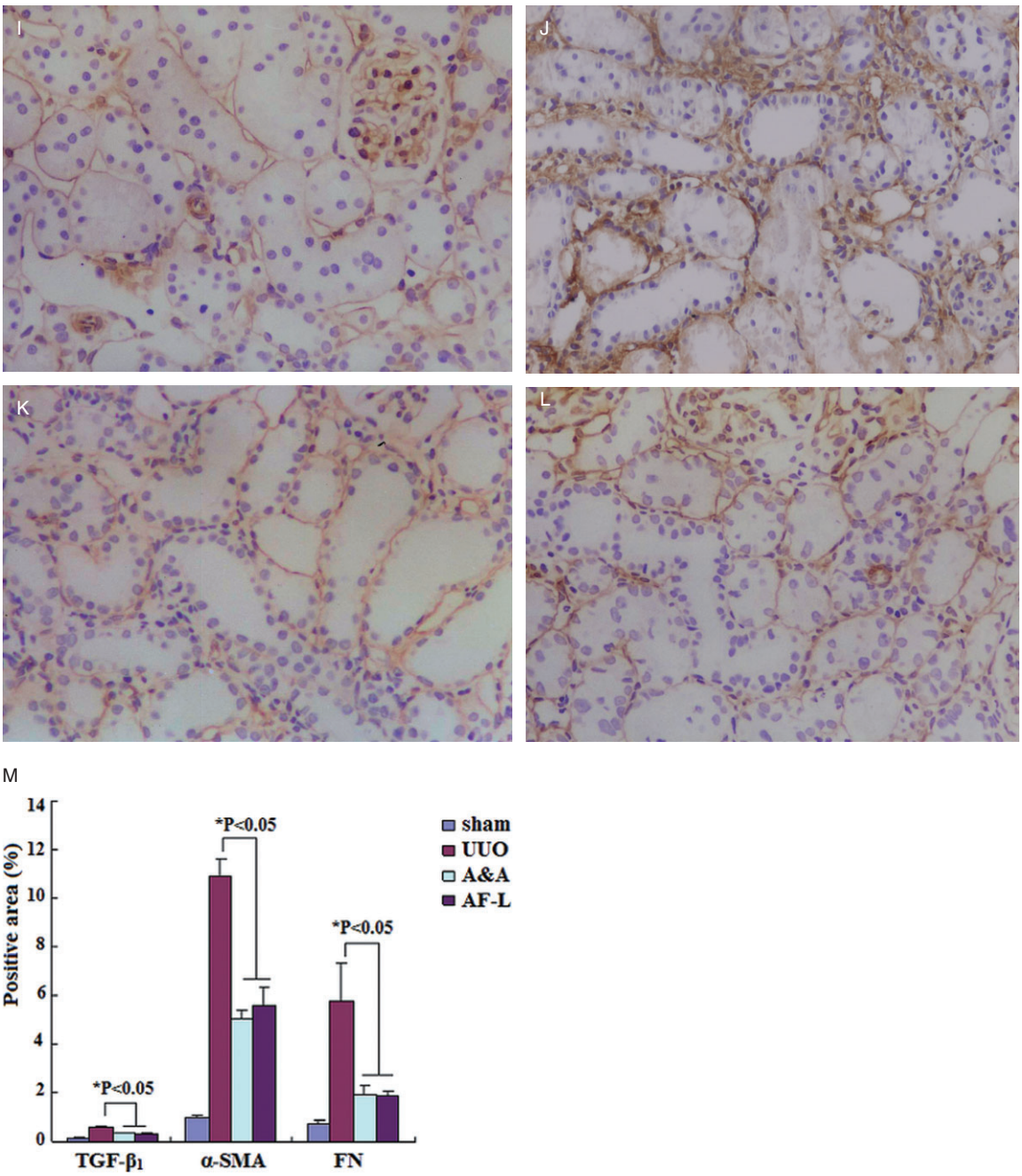

Figure 2
Continued.

of the epithelial cells. As shown in Figures 8 and 9, IL-1β significantly increased α-SMA and fibronectin expression in HK-2 cells ($P < 0.05$). *AF* not only decreased the basal expression of α-SMA and fibronectin in HK-2 cells but also significantly inhibited the expression of α-SMA and fibronectin in IL-1β-induced cells ($P < 0.05$). Monotherapy with AS-IV or FA of HK-2 cells had no effect on the expression of α-SMA and fibronectin in either basal conditions or after IL-1β stimulation. It was also shown that *AF* inhibits the expression of α-SMA and fibronectin mRNA in HK-2 cells stimulated with IL-1β ($P < 0.05$; Figures 10 and 11).

We further examined whether *AF* decreased EMT through the main MAPK signalling pathway, including JNK, extracellular signal-regulated kinases (ERK) and P38. IL-1β significantly increased JNK, ERK and P38 phosphorylation, but *AF* only significantly inhibited IL-1β-induced JNK phosphorylation ($P < 0.05$, Figure 12), with no effect on ERK or P38 phosphorylation (data not shown).

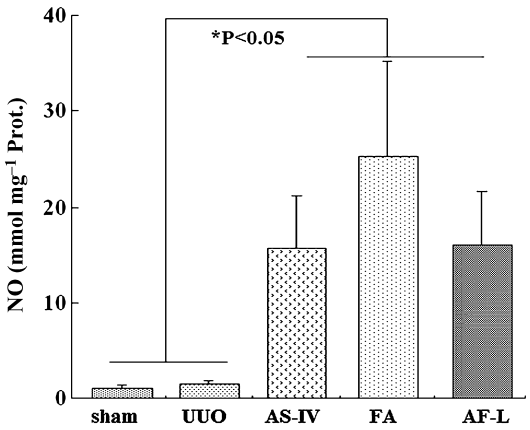

Figure 3

The production of NO in the obstructed kidneys. UUO: unilateral ureteral obstruction, AS-IV: astragaloside IV, FA: ferulic acid, *AF*-L: AS-IV and FA (low dosage). AS-IV and FA dramatically increased the production of NO in obstructed kidneys ($P < 0.05$). NO production was expressed as μmol·mg^{-1} protein of NO_2^- in the tissue. Values are mean ± SEM. *$P < 0.05$ versus UUO kidneys.

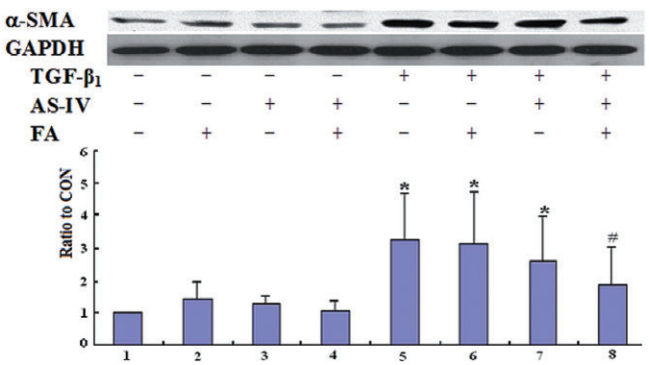

Figure 4

The expression of α-SMA in NRK-49F cells. AS-IV: astragaloside IV, FA: ferulic acid, *AF*: AS-IV and FA. *AF* decreased the expression of α-SMA in TGF-β_1-treated cells ($P < 0.05$), but AS-IV or FA alone had not effect α-SMA expression. Values are mean ± SEM. *$P < 0.05$ versus DMSO-treated cells, #$P < 0.05$ versus TGF-β_1-treated cells.

AF alleviated the expression of p-JNK in obstructed kidneys

Concomitant with the increased activity of JNK, the expression of p-JNK was confirmed in obstructed kidneys using immunofluorescence. Normally, p-JNK is localized to some tubular epithelial cells and occasional glomerular cells. UUO induced a marked increase in JNK phosphorylation with p-JNK staining prominent in dilated tubules, as well as in interstitial cells. *AF* alleviated the expression of p-JNK (Figure 13).

Discussion and conclusions

In this study, we examined the renoprotective effects of AS-IV and FA, two active constituents of a mixture of Astragali

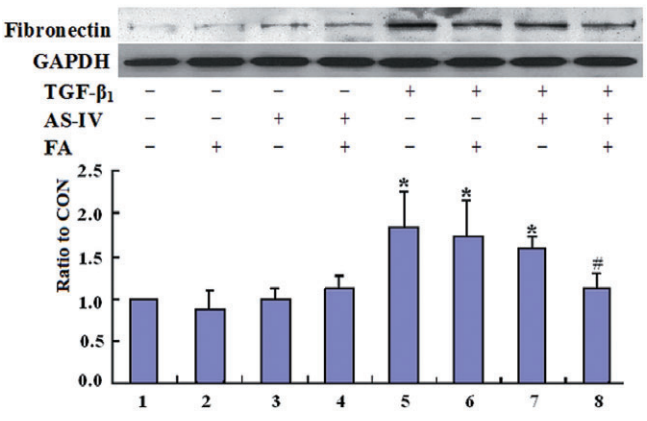

Figure 5

The expression of fibronectin in NRK-49F cells. AS-IV: astragaloside IV, FA: ferulic acid, *AF*: AS-IV and FA. *AF* decreased the expression of fibronectin in TGF-β_1-treated cells ($P < 0.05$), but AS-IV or FA had no effect on fibronectin expression. Values are mean ± SEM. *$P < 0.05$ versus DMSO-treated cells, #$P < 0.05$ versus TGF-β_1-treated cells.

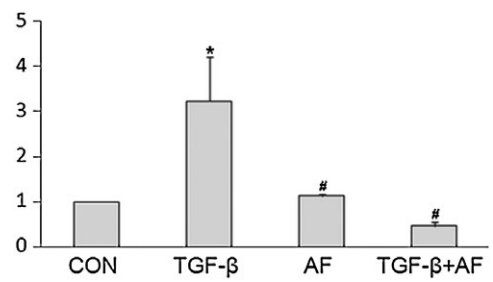

Figure 6

The expression of α-SMA mRNA in NRK-49F cells. AS-IV: astragaloside IV, FA: ferulic acid, *AF*: AS-IV and FA. *AF* decreased the expression of α-SMA mRNA in TGF-β_1-treated cells ($P < 0.05$). Values are mean ± SEM. *$P < 0.05$ versus control (DMSO-treated cells), #$P < 0.05$ versus TGF-β_1-treated cells.

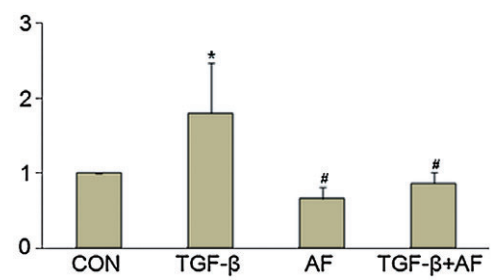

Figure 7

The expression of fibronectin mRNA in NRK-49F cells. AS-IV: astragaloside IV, FA: ferulic acid, *AF*: AS-IV and FA. *AF* decreased the expression of fibronectin mRNA in TGF-β_1-treated cells ($P < 0.05$). Values are mean ± SEM. *$P < 0.05$ versus control, #$P < 0.05$ versus TGF-β_1-treated cells.

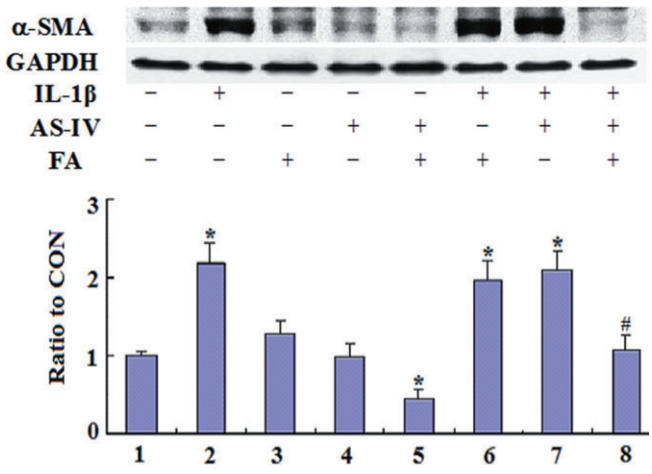

Figure 8

The expression of α-SMA in HK-2 cells. AS-IV: astragaloside IV, FA: ferulic acid, *AF*: AS-IV and FA. *AF* decreased the expression of α-SMA in IL-1β-treated cells ($P < 0.05$). Values are mean ± SEM. *$P < 0.05$ versus DMSO-treated cells, #$P < 0.05$ versus IL-1β-treated cells.

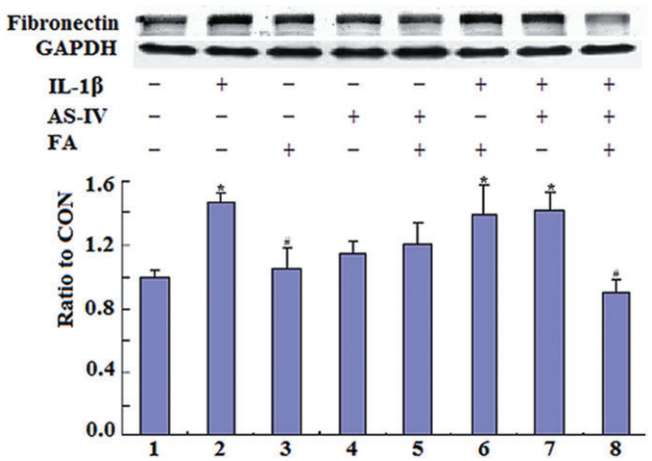

Figure 9

The expression of fibronectin in HK-2 cells. AS-IV: astragaloside IV, FA: ferulic acid, *AF*: AS-IV and FA. *AF* decreased the expression of fibronectin in IL-1β-treated cells ($P < 0.05$). Values are mean ± SEM. *$P < 0.05$ versus DMSO-treated cells, #$P < 0.05$ versus IL-1β-treated cells.

Radix and Angelicae Sinensis Radix, which has been shown to inhibit the progression of renal fibrosis and improve renal function in several animal models of kidney diseases (Li *et al.*, 1998; Wang *et al.*, 2004; Zhang *et al.*, 2006b; Meng *et al.*, 2007). The result indicated that the combination of AS-IV and FA (*AF*) have renoprotective effects characterized by a decrease in serum creatinine and urea, and a reduction in tubulointerstitial fibrosis in obstructive nephropathy, even though neither AS-IV nor FA alone attenuated renal injury. Renal interstitial fibrosis is widely accepted as being closely associated with the deterioration of renal function because the tubulointerstitium comprises about 90% of the volume of

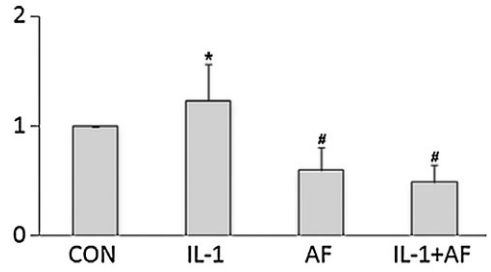

Figure 10

The expression of α-SMA mRNA in HK-2 cells. AS-IV: astragaloside IV, FA: ferulic acid, *AF*: AS-IV and FA. *AF* decreased the expression of α-SMA mRNA in IL-1β-treated cells ($P < 0.05$). Values are mean ± SEM. *$P < 0.05$ versus control (DMSO-treated cells), #$P < 0.05$ versus IL-1β-treated cells.

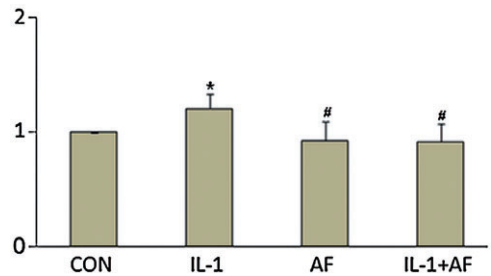

Figure 11

The expression of fibronectin mRNA in HK-2 cells. AS-IV: astragaloside IV, FA: ferulic acid, *AF*: AS-IV and FA. *AF* decreased the expression of fibronectin mRNA in IL-1β-treated cells ($P < 0.05$). Values are mean ± SEM. *$P < 0.05$ versus control, #$P < 0.05$ versus IL-1β-treated cells.

the kidney (Bohle *et al.*, 1987). The prevention of interstitial fibrosis can significantly slow the progression of kidney disease. Thus, the combination of AS-IV and FA might be beneficial to the injured kidney.

UUO is recognized as an ideal experimental model of renal interstitial fibrosis. Ureteral obstruction leads to a significant reduction in renal blood flow, local ischaemia/hypoxia and an inflammatory response, followed by renal interstitial myofibroblast proliferation and ECM accumulation in the renal interstitium (Chevalier *et al.*, 2009). In the process of renal fibrosis, the overexpression of profibrotic cytokines (e.g. TGF-β_1, CTGF) and inflammatory factors (such as IL-β, TNF) contributes to kidney damage.

Notably, the proliferation of myofibroblasts in renal tubulointerstitium is the crucial event in the progression of renal fibrosis. The activation of resident fibroblasts results in a massive increase in the number of myofibroblasts during the early stage of obstructive nephropathy. From day 7 after ureteral obstruction, the transdifferentiation of epithelial and endothelial cells becomes the major source of myofibroblasts (Grande *et al.*, 2009). TGF-β_1 plays a critical role in the initiation and progression of renal fibrosis (Qi *et al.*, 2008). In response to TGF-β_1, resident fibroblasts can be activated (Suzuki *et al.*, 2004), and tubular epithelial cells can transdifferentiate into myofibroblasts (Sebe *et al.*, 2008). IL-1β

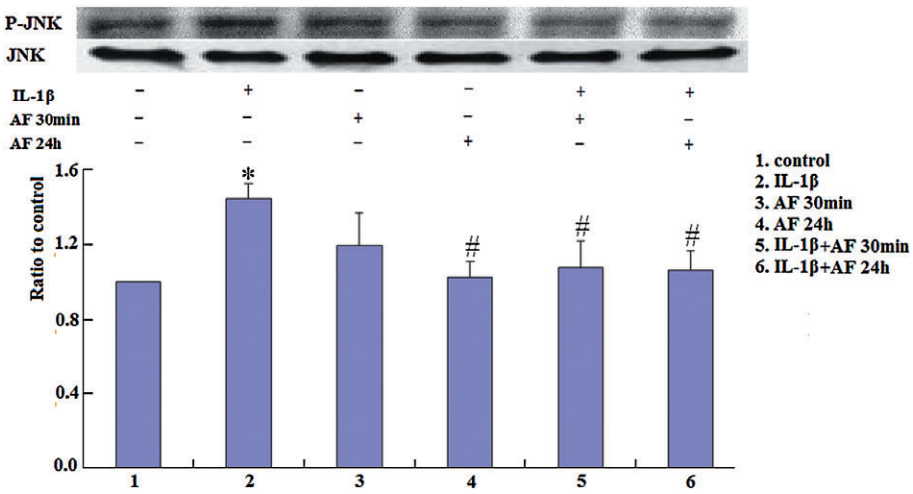

Figure 12

The expression of JNK in HK-2 cells. AS-IV: astragaloside IV, FA: ferulic acid, *AF*: AS-IV and FA. *AF* decreased JNK phosphorylation in IL-1β-treated cells ($P < 0.05$). Values are mean ± SEM. *$P < 0.05$ versus DMSO-treated cells, #$P < 0.05$ versus IL-1β-treated cells.

promotes tubulointerstitial fibrosis by impairing proximal tubule cells, inhibiting growth, α-SMA expression and fibronectin production, which are mediated by a TGF-β_1-dependent mechanism (Fan *et al.*, 2001). In this study, we investigated the effects of AS-IV and FA on two of the main sources of myofibroblasts, fibroblasts and renal tubular epithelial cells. Although treatment with either AS-IV or FA alone had no effect, the combination of the two constituents (*AF*) significantly reduced the expression of α-SMA and fibronectin in activated fibroblasts and tubular epithelial cells. *AF* is thought to reduce the production of ECM resulting in the inhibition of myofibroblast proliferation.

The activation of MAPK signalling is an important pathway in TGF-β_1-mediated renal fibrosis (Böttinger *et al.*, 2002). The three phosphorylation cascades of MAPKs pathway, including ERK, JNK and p38 MAPK, participate in TGF-β_1 signalling cascades. These kinases can be activated by growth factors and environmental stress leading to alterations in cell growth and other key cell functions, such as EMT (Rodrigues-Díez *et al.*, 2008). Recently, JNK signalling was reported to be involved in TGF-β_1-induced EMT in tubular epithelial cells (Mariasegaram *et al.*, 2010). In other epithelial cell types, including tracheal epithelial cells and keratinocytes, TGF-β_1 also induces EMT via JNK signalling (Alcorn *et al.*, 2008; Santibañez *et al.*, 2006). In this study, the inhibition of α-SMA and fibronectin by *AF* was found to be associated with the JNK pathway in the TGF-β_1-treated NRK-49F and IL-β-treated HK-2 cells. Thus, the activation of JNK signalling may be an important pathway through which *AF* induces an antifibrotic effect in renal tubulointerstitial fibrosis.

AS-IV and FA have been found to inhibit the MAPK pathway in several studies by other researchers. Either AS-IV or FA was found to block the JNK pathway, but the doses used in these experiments were higher than those used in the present study. However, JNK activity is differentially regulated by various protein kinases, including MKK4 and MKK7 (Fleming *et al.*, 2000), mixed lineage kinases (Hirai *et al.*, 1997) and TGF-activated protein kinase 1 (Wang *et al.*, 1997). JNK1 activity has also been shown to be up-regulated as a consequence of proteolytic cleavage of $p21^{WAF1/CIP1}$ (Shim *et al.*, 1996), and Ca^{2+} and reactive oxygen species (ROS) generation play an important role in the activation of the JNK pathway (Ham *et al.*, 2006). AS-IV has been found to reduce the increase in ROS (Xu *et al.*, 2008), as well as prevent the rise in intracellular [Ca^{2+}] (Hu *et al.*, 2009). Also, FA was shown to elevate the protein content of the JNK1 inhibitor $p21^{WAF1/CIP1}$ (Hou *et al.*, 2004). However, these effects of either AS-IV or FA alone are not enough to inhibit the activation of JNK at the doses used in our study, but when the actions of these two compounds are combined, a synergistic effect is produced that blocks the JNK pathway, induced by inhibition of JNK activation and cleavage.

Our study also demonstrated that AS-IV and FA (*AF*) increased NO production in the kidney. NO has been also shown to ameliorate renal injury in kidney diseases (Trachtman *et al.*, 1995; Huang *et al.*, 2000). AS-IV has been reported to enhance the activation of endothelial NO synthase (Zhang *et al.*, 2007), and FA has been shown to decrease oxidative stress (Ma *et al.*, 2010). Thus, *AF* not only increases eNOS activation but also protects NO by increasing the activity of scavenging ROS; these effects converge to increase NO production and so promote the remission of interstitial fibrosis.

Unfortunately, the positive role of AS-IV or FA alone on renal fibrosis was not observed at the doses of AS-IV or FA used in this study. Higher doses were not used because the range of concentrations of AS-IV or FA detected by HPLC method was limited by the concentrations of Astragali Radix and Angelicae Sinensis Radix available. Therefore, further studies needed to observe the effects of AS-IV and FA at different concentrations and to identify any other active components in Astragali Radix and Angelicae Sinensis Radix with renoprotective effects.

The mechanisms of renal fibrosis are associated with a series of dynamic pathological changes in the progression of renal injury. In this study, we demonstrated that *AF* possesses

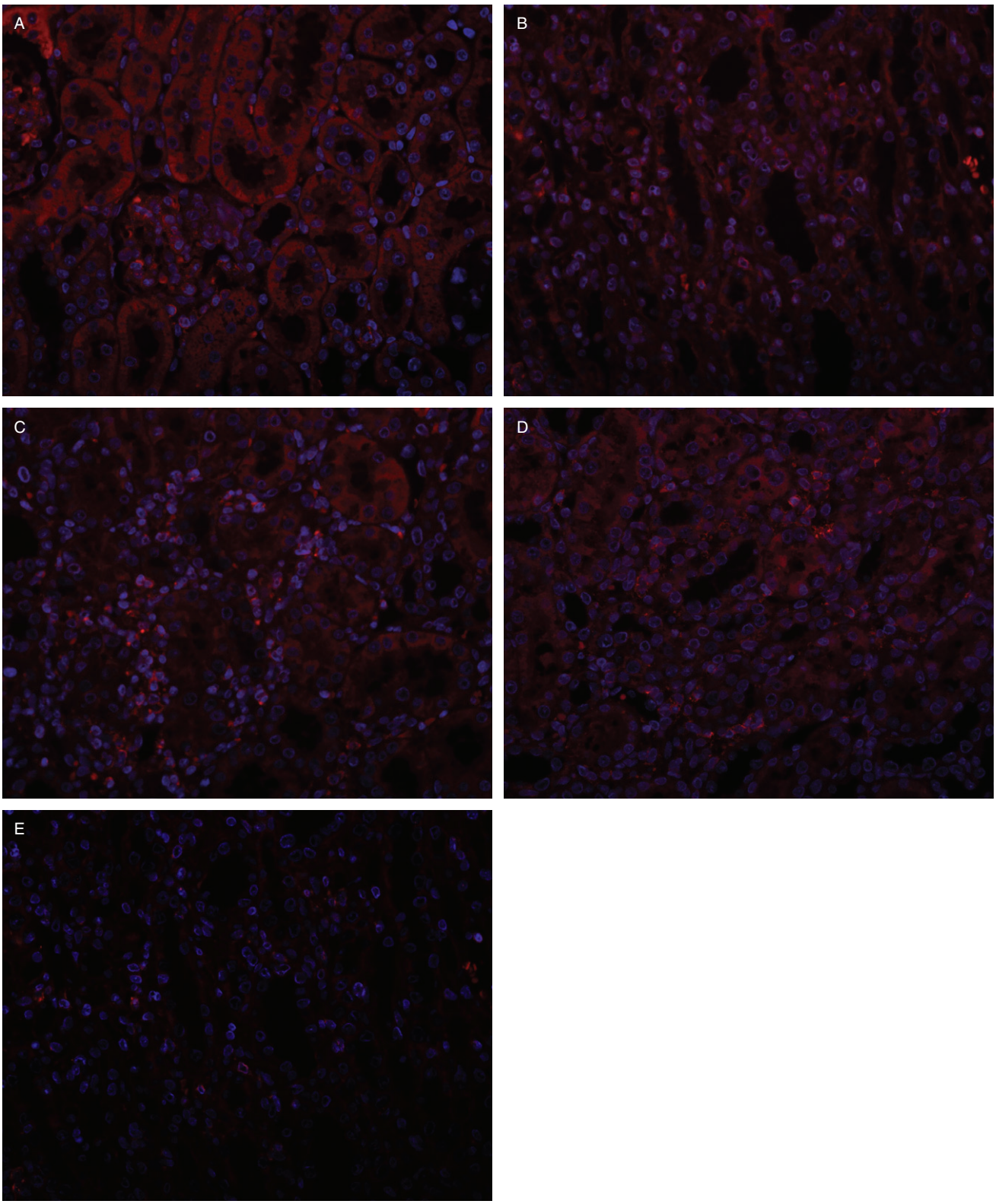

Figure 13

The expression of p-JNK in obstructed kidneys (immunofluorescence, 200×). (A) p-JNK in sham group. (B) p-JNK in UUO group. (C) p-JNK in AS-IV treatment group. (D) p-JNK in FA treatment group. (E) p-JNK in AF-L treatment group. UUO: unilateral ureteral obstruction, AS-IV: astragaloside IV, FA: ferulic acid, AF: AS-IV & FA.

antifibrotic, which are characterized by a decrease in cellular infiltration, tubular atrophy and interstitial fibrosis, as well as inhibition of FN, α-SMA and TGF-β_1 activity. Fibroblasts and tubular epithelial cells are two important sources of myofibroblasts; *in vitro* experiments were employed to explore the potential cellular mechanisms of *AF*, but the cellular experiments only demonstrated a small part of the complicated process. Thus, we cautiously conclude that *AF* can alleviate renal tubulointerstitial fibrosis, and this is associated with inhibition of tubular EMT and fibroblast activation, as well as an increase in NO production in the kidney.

Acknowledgements

The experimental work was supported by the Key Program of the National Natural Science Foundation of China (No. 30330710) and the Specialized Research Fund for the Doctoral Program of Higher Education (No. 20070001761).

Conflicts of interest

No.

References

Alcorn JF, Guala AS, van der Velden J, McElhinney B, Irvin CG, Davis RJ *et al.* (2008). Jun N-terminal kinase 1 regulates epithelial-to-mesenchymal transition induced by TGF-beta1. J Cell Sci 121: 1036–1045.

Bohle A, Mackensen-Haen S, von Gise H (1987). Significance of tubulointerstitial changes in the renal cortex for the excretory function and concentration ability of the kidney: a morphometric contribution. Am J Nephrol 7: 421–433.

Böttinger EP, Bitzer M (2002). TGF-beta signaling in renal disease. J Am Soc Nephrol 13: 2600–2610.

Chen J, Gui D, Chen Y, Mou L, Liu Y, Huang J (2008). Astragaloside IV improves high glucose-induced podocyte adhesion dysfunction via alpha3beta1 integrin upregulation and integrin-linked kinase inhibition. Biochem Pharmacol 76: 796–804.

Chen XM, Qi W, Pollock CA (2009). CTGF and chronic kidney fibrosis. Front Biosci (Schol Ed) 1: 132–141.

Chevalier RL, Forbes MS, Thornhill BA (2009). Ureteral obstruction as a model of renal interstitial fibrosis and obstructive nephropathy. Kidney Int 75: 1145–1152.

Fan JM, Huang XR, Ng YY, Nikolic-Paterson DJ, Mu W, Atkins RC *et al.* (2001). Interleukin-1 induces tubular epithelial-myofibroblast transdifferentiation through a transforming growth factor-beta1-dependent mechanism in vitro. Am J Kidney Dis 37: 820–831.

Fleming Y, Armstrong CG, Morrice N, Paterson A, Goedert M, Cohen P (2000). Synergistic activation of stress-activated protein kinase 1/c-Jun N-terminal kinase (SAPK1/JNK) isoforms by mitogen-activated protein kinase kinase 4 (MKK4) and MKK7. Biochem J 352: 145–154.

Fujita A, Sasaki H, Doi A, Okamoto K, Matsuno S, Furuta H *et al.* (2008). Ferulic acid prevents pathological and functional abnormalities of the kidney in Otsuka Long-Evans Tokushima Fatty diabetic rats. Diabetes Res Clin Pract 79: 11–17.

Gaedeke J, Noble NA, Border WA (2002). Angiotensin II and progressive renal insufficiency. Curr Hypertens Rep 4: 403–407.

Grande MT, López-Novoa JM (2009). Fibroblast activation and myofibroblast generation in obstructive nephropathy. Nat Rev Nephrol 5: 319–328.

Ham YM, Lim JH, Na HK, Choi JS, Park BD, Yim H *et al.* (2006). Ginsenoside-Rh2-induced mitochondrial depolarization and apoptosis are associated with reactive oxygen species- and Ca2+-mediated c-Jun NH2-terminal kinase 1 activation in HeLa cells. J Pharmacol Exp Ther 319: 1276–1285.

Hewitson TD (2009). Renal tubulointerstitial fibrosis: common but never simple. Am J Physiol Renal Physiol 296: F1239–F1244.

Hirai S, Katoh M, Terada M, Kyriakis JM, Zon LI, Rana A *et al.* (1997). MST/MLK2, a member of the mixed lineage kinase family, directly phosphorylates and activates SEK1, an activator of c-Jun N-terminal kinase/stress-activated protein kinase. J Biol Chem 272: 15167–15173.

Hou YZ, Yang J, Zhao GR, Yuan YJ (2004). Ferulic acid inhibits vascular smooth muscle cell proliferation induced by angiotensin II. Eur J Pharmacol 499: 85–90.

Hu JY, Han J, Chu ZG, Song HP, Zhang DX, Zhang Q *et al.* (2009). Astragaloside IV attenuates hypoxia-induced cardiomyocyte damage in rats by upregulating superoxide dismutase-1 levels. Clin Exp Pharmacol Physiol 36: 351–357.

Huang A, Palmer LS, Hom D, Valderrama E, Trachtman H (2000). The role of nitric oxide in obstructive nephropathy. J Urol 163: 1276–1281.

Kalluri R, Neilson EG (2003). Epithelial-mesenchymal transition and its implications for fibrosis. J Clin Invest 112: 1776–1184.

Li L, Chen M, Tong T, Wang H (1998). The molecular basis of Chinese herbs (Astragali and Angelica) on increasing serum albumin synthesis in nephrotic rats. Nephrology (Carlton) 4: 373–378.

Li X, Wang H (2005). Chinese herbal medicine in the treatment of chronic kidney disease. Adv Chronic Kidney Dis 12: 276–281.

Lin SL, Kisseleva T, Brenner DA, Duffield JS (2008). Pericytes and perivascular fibroblasts are the primary source of collagen-producing cells in obstructive fibrosis of the kidney. Am J Pathol 173: 1617–1627.

Ma ZC, Hong Q, Wang YG, Tan HL, Xiao CR, Liang QD *et al.* (2010). Ferulic acid protects human umbilical vein endothelial cells from radiation induced oxidative stress by phosphatidylinositol 3-kinase and extracellular signal-regulated kinase pathways. Biol Pharm Bull 33: 29–34.

Mariasegaram M, Tesch GH, Verhardt S, Hurst L, Lan HY, Nikolic-Paterson DJ (2010). Lefty antagonises TGF-beta1 induced epithelial-mesenchymal transition in tubular epithelial cells. Biochem Biophys Res Commun 393: 855–859.

Meng L, Qu L, Tang J, Cai SQ, Wang H, Li X (2007). A combination of Chinese herbs, Astragalus membranaceus var. mongholicus and Angelica sinensis, enhanced nitric oxide production in obstructed rat kidney. Vascul Pharmacol 47: 174–183.

Meng L, Van Putten V, Qu L, Nemenoff RA, Shang MY, Cai SQ *et al.* (2010). Altered expression of genes profiles modulated by a combination of Astragali Radix and Angelicae Sinensis Radix in obstructed rat kidney. Planta Med 76: 1431–1438.

Peng A, Gu Y, Lin SY (2005). Herbal treatment for renal diseases. Ann Acad Med Singapore 34: 44–51.

Qi W, Chen X, Poronnik P, Pollock CA (2006). The renal cortical fibroblast in renal tubulointerstitial fibrosis. Int J Biochem Cell Biol 38: 1–5.

Qi W, Chen X, Poronnik P, Pollock CA (2008). Transforming growth factor-beta/connective tissue growth factor axis in the kidney. Int J Biochem Cell Biol 40: 9–13.

Qu YZ, Li M, Zhao YL, Zhao ZW, Wei XY, Liu JP *et al.* (2009). Astragaloside IV attenuates cerebral ischemia-reperfusion-induced increase in permeability of the blood-brain barrier in rats. Eur J Pharmacol 606: 137–141.

Radford MG Jr, Donadio JV Jr, Bergstralh EJ, Grande JP (1997). Predicting renal outcome in IgA nephropathy. J Am Soc Nephrol 8: 199–207.

Ripley E (2009). Complementary effects of angiotensin-converting enzyme inhibitors and angiotensin receptor blockers in slowing the progression of chronic kidney disease. Am Heart J 157: S7–S16.

Rodrigues-Díez R, Carvajal-González G, Sánchez-López E, Rodríguez-Vita J, Rodrigues Díez R, Selgas R *et al.* (2008). Pharmacological modulation of epithelial mesenchymal transition caused by angiotensin II. Role of ROCK and MAPK pathways. Pharm Res 25: 2447–2461.

Santibañez JF (2006). JNK mediates TGF-beta1-induced epithelial mesenchymal transdifferentiation of mouse transformed keratinocytes. FEBS Lett 580: 5385–5391.

Schnaper HW, Jandeska S, Runyan CE, Hubchak SC, Basu RK, Curley JF *et al.* (2009). TGF-beta signal transduction in chronic kidney disease. Front Biosci 14: 2448–2465.

Sebe A, Leivonen SK, Fintha A, Masszi A, Rosivall L, Kähäri VM *et al.* (2008). Transforming growth factor-beta-induced alpha-smooth muscle cell actin expression in renal proximal tubular cells is regulated by p38beta mitogen-activated protein kinase, extracellular signal-regulated protein kinase1,2 and the Smad signalling during epithelial-myofibroblast transdifferentiation. Nephrol Dial Transplant 23: 1537–1545.

Shim J, Lee H, Park J, Kim H, Choi EJ (1996). A non-enzymatic p21 protein inhibitor of stress-activated protein kinases. Nature 381: 804–806.

Song J, Meng L, Li S, Qu L, Li X (2009). A combination of Chinese herbs, Astragalus membranaceus var. mongholicus and Angelica sinensis, improved renal microvascular insufficiency in 5/6 nephrectomized rats. Vascul Pharmacol 50: 185–193.

Strutz F, Zeisberg M (2006). Renal fibroblasts and myofibroblasts in chronic kidney disease. J Am Soc Nephrol 17: 2992–2998.

Suzuki H, Uchida K, Nitta K, Nihei H (2004). Role of mitogen-activated protein kinase in the regulation of transforming growth factor-beta-induced fibronectin accumulation in cultured renal interstitial fibroblasts. Clin Exp Nephrol 8: 188–195.

Trachtman H, Futterweit S, Singhal P (1995). Nitric oxide modulates the synthesis of extracellular matrix proteins in cultured rat mesangial cells. Biochem Biophys Res Commun 207: 120–125.

Vesey DA, Cheung CW, Cuttle L, Endre ZA, Gobé G, Johnson DW (2002). Interleukin-1beta induces human proximal tubule cell injury, alpha-smooth muscle actin expression and fibronectin production. Kidney Int 62: 31–40.

Wang H, Li J, Yu L, Zhao Y, Ding W (2004). Antifibrotic effect of the Chinese herbs, Astragalus mongholicus and Angelica sinensis, in a rat model of chronic puromycin aminonucleoside nephrosis. Life Sci 74: 1645–1658.

Wang W, Zhou G, Hu MC, Yao Z, Tan TH (1997). Activation of the hematopoietic progenitor kinase-1 (HPK1)-dependent, stress-activated c-Jun N-terminal kinase (JNK) pathway by transforming growth factor beta (TGF-beta)-activated kinase (TAK1), a kinase mediator of TGF beta signal transduction. J Biol Chem 272: 22771–22775.

Wojcikowski K, Johnson DW, Gobe G (2006). Herbs or natural substances as complementary therapies for chronic kidney disease: ideas for future studies. J Lab Clin Med 147: 160–166.

Xiao HB, Liang XM, Lu PZ, Chen ZJ (1999). New analysis methodology and application for Chinese prescription (Chinese). Chin Sci Bull 44: 588–596.

Xu ME, Xiao SZ, Sun YH, Ou-Yang Y, Zheng XX (2006). Effects of astragaloside IV on pathogenesis of metabolic syndrome in vitro. Acta Pharmacol Sin 27: 229–236.

Xu XL, Chen XJ, Ji H, Li P, Bian YY, Yang D *et al.* (2008). Astragaloside IV improved intracellular calcium handling in hypoxia-reoxygenated cardiomyocytes via the sarcoplasmic reticulum Ca-ATPase. Pharmacology 81: 325–332.

Zeisberg EM, Potenta SE, Sugimoto H, Zeisberg M, Kalluri R (2008). Fibroblasts in kidney fibrosis emerge via endothelial-to-mesenchymal transition. J Am Soc Nephrol 19: 2282–2287.

Zhang C, Wang XH, Zhong MF, Liu RH, Li HL, Zhang WD *et al.* (2007). Mechanisms underlying vasorelaxant action of astragaloside IV in isolated rat aortic rings. Clin Exp Pharmacol Physiol 34: 387–392.

Zhang M, Tang J, Li X (2005). Interleukin-1beta-induced transdifferentiation of renal proximal tubular cells is mediated by activation of JNK and p38 MAPK. Nephron Exp Nephrol 99: e68–e76.

Zhang YW, Xie D, Chen YX, Zhang HY, Xia ZX (2006a). Protective effect of Gui Qi mixture on the progression of diabetic nephropathy in rats. Exp Clin Endocrinol Diabetes 114: 563–568.

Zhang YW, Xie D, Xia B, Zhen RT, Liu IM, Cheng JT (2006b). Suppression of transforming growth factor-beta1 gene expression by Danggui buxue tang, a traditional Chinese herbal preparation, in retarding the progress of renal damage in streptozotocin- induced diabetic rats. Horm Metab Res 38: 82–88.

Zhao J, Shang MY, Meng L, Rong S, Ma C, Qu L *et al.* (2010). Screening Effective parts of a combination of Astragali Radix and Angelicae Sinensis Radix (A&A) for its renoprotective effects. Zhongguo Zhong Yao Za Zhi 35: 2893–2898 [Chinese].